Experimental and numerical investigations of the Czochralski growth of Li2MoO4 crystals for heat-scintillation cryogenic bolometers

C. Stelian, M. Velazquez, Philippe Veber, A Ahmine, T. Duffar, P. de Marcillac, A. Giuliani, D. Poda, S. Marnieros, C. Nones, et al.

Experimental and numerical investigations of the Czochralski growth of Li_2MoO_4 crystals for heat-scintillation cryogenic bolometers

C. Stelian[1], M. Velazquez[1,*], P. Veber[2], A. Ahmine[1], T. Duffar[1], P. de Marcillac[3], A. Giuliani[3,4], D. V. Poda[3,5], S. Marnieros,[3] C. Nones[6], V. Novati[3], E. Olivieri[3], A. S. Zolotarova[3], H. Cabane[7], T. Redon[3]

[1]*Univ. Grenoble Alpes, CNRS, Grenoble INP, SIMAP, 38000 Grenoble, France*

[2]*Université Lyon, Université Claude Bernard Lyon 1, CNRS, Institut Lumière Matière UMR 5306, 69100, Villeurbanne, France*

[3]*CSNSM, Univ. Paris-Sud, CNRS/IN2P3, Université Paris-Saclay, 91405 Orsay, France*

[4]*DISAT, Università dell'Insubria, 22100 Como, Italy*

[5]*Institute for Nuclear Research, 03028 Kyiv, Ukraine*

[6]*IRFU, CEA, Université Paris-Saclay, F-91191 Gif-sur-Yvette, France*

[7]*CristalInnov, Cleanspace 354 Voie Magellan, Sainte-Hélène du Lac, 73800, France*

*Corresponding author: Matias.Velazquez@simap.grenoble-inp.fr

Abstract

A new technology for the mass production of lithium molybdate (Li_2MoO_4) crystals needed for the realization of the cryogenic neutrinoless double-beta decay detectors is under development within the framework of the CLYMENE project. Crystals with 4 and 5 cm in diameter were grown in two different Czochralski configurations. The first configuration, based on inductive heating of a RF coil coupled with a platinum crucible, was used to grow crystals of 4 cm in diameter. Bolometric tests performed with two samples cut from a 230 g crystal have shown less performances of the large sample (158 g), which had a cleavage, as compared to the small non-cracked sample (13.5 g). Numerical

modeling was applied to investigate the temperature field in the furnace, the melt convection and thermo-elastic stresses in the crystal. Numerical results reveal 30% higher thermal stress at the bottom part of the ingot in the case of a concave shape of the crystal tail (experimental case) as compared to the case of a convex shaped tail. This could explain why the fracture started at the bottom part of the 230 g crystal boule, and highlights the importance of the crystal shape in the last stage of growth process. The furnace configuration used to grow 5 cm-diameter crystals was numerically optimized in order to reduce the thermal stress in the crystals. The first kg-mass Li_2MoO_4 ingot grown in the optimized configuration exhibit regular shape and good structural quality.

Keywords: A1. Computer simulation, A2. Czochralski method, B1. Lithium compounds, B1. Oxides, B2. Scintillator materials.

1. Introduction

Li_2MoO_4 (LMO) crystals are among the best candidates for the next generation of tonne-scale bolometric experiments aiming at detecting neutrinoless double-beta decays [1,2]. The goal of the CLYMENE project is to develop an optimized Czochralski pulling technology for the production of large-mass high quality LMO crystals [3]. So far, the most common defects found in the crystals grown by the Czochralski technique are cracks and inclusions. Bolometric tests performed with two samples (cracked and non-cracked) cut from a 230 g LMO crystal, have demonstrated the better performances of detector built with the small non-cracked crystal (13.5 g) as compared to the detector built with the large size (158 g) cracked crystal [4].

In this work, the growth of large size Li_2MoO_4 crystals is investigated by means of experiments and numerical modeling. The furnace configuration used to grow kg-mass LMO ingots is numerically

optimized in order to reduce the thermal stresses in the crystals, which are likely to induce crack formation in the zone just above the tail.

2. Model description

The equations describing the heat transfer, fluid flow and thermal stresses are solved by using the commercial code *COMSOL Multiphysics*. 2D axisymmetric global modeling was first applied to compute the temperature field in the furnace and the flow in the melt at different stages of the growth process. The shape of the crystal-melt interface was computed by using the deformable mesh technique. The heat transfer computations include thermal exchanges by conduction and radiation. The internal radiation in the semi-transparent LMO crystal is computed by applying the P1-approximation model. The flow computations include buoyancy convection, Marangoni flow and forced convection generated by the crystal rotation at 5 rpm. The temperatures carried out from the global modeling are used to perform 3D local modeling of thermal stress in the crystal. Three-dimensional stress computations take into account the anisotropic elastic properties of Li_2MoO_4, which belongs to the $R\bar{3}$ space group. The values of the independent elastic constants calculated in the coordinate system xyz (where the x-axis is parallel to the a-axis and the z-axis parallel to the c-axis of LMO) are given by: C_{11}=58.9 GPa, C_{33}=78.8 GPa, C_{44}=15.9 GPa, C_{12}=25.2 GPa, C_{13}=15.6 GPa, C_{14}=0.46 GPa, C_{15}=0.18 GPa [5]. The growth direction was considered parallel to the y-axis. More details about modeling Czochralski growth of Li_2MoO_4 crystals are given in our previous work [6].

3. Results and discussion

3.1 Crystals of 4 cm in diameter

Several LMO crystals of 4 cm in diameter were grown in an inductive Czochralski furnace [3]. The growth was performed in a platinum crucible at low pulling and rotation rates (0.6 mm/h and 5 rpm). The larger mass ingot (230 g) grown in this configuration had 6 cm in length (cylindrical part) and an average diameter of 4 cm (Fig. 1a). The ingot tail has an unusual shape since the growth was performed without automatic control of the crystal shape. The photograph of the crystal boule before cutting shows a concave shape of the lateral surface of the tail (Fig. 1a). The crystal cracked during the cutting of its bottom part (Fig. 1b). The performance of two scintillating bolometers (158 g cracked and 13.5 g non-cracked samples) cut from this ingot were investigated in a previous work [4]. The large-mass (158 g) cracked crystal revealed a shorter response time and a decrease of both the FWHM resolution and the sensitivity by a factor of 17 and 70, respectively, as compared to the small (13.5 g) non-cracked crystal.

Results carried out from simulations of the final stage of the growth process (length of the cylindrical part of the crystal $L_{cyl} = 6$ cm) are shown in Fig. 2. The computed temperatures in the furnace (left side) and the velocity field in the melt (right side) are shown in Fig. 2a. The blue line represents the solidification isotherm. It is found that the solid-liquid interface is convex shaped (seen from the liquid) with a large curvature. The computed interface deflection is f=1.2 cm. The isotherms are very curved at the bottom part of the crystal. This generates large radial temperature gradients and significant thermal stresses in the LMO ingot. The maximum radial temperature gradient is located near the triple solid-liquid-gas point: G_{rad}=220 K.cm^{-1}. Figure 2b shows the von Mises stress distribution at the outer surface of the crystal. Higher stress is located at the bottom part of the ingot. The stress is non-symmetrically distributed, with a maximum in the x-y plane (c-plane) near the triple solid-liquid-gas line.

Figure 3 shows the von Mises stress distribution in the longitudinal x-y section of the ingot at the end stage of the growth (solidification length $L = 6.3$ cm). The height of the crystal tail is 0.3 cm. Two cases were numerically investigated: the case with a convex shape of the lateral surface of the tail (Fig. 3a) and the case with a concave shape of the tail (Fig. 3b). Computations show that the maximum stress increases by 30% in the case with a concave shape of the tail (the experimental case). This could explain why the fracture started at the bottom of the cylindrical part of the ingot when the crystal boule was cut (see the photograph in Fig. 3b). Therefore, it is found that the shape of the crystal tail influences the thermo-elastic stresses and the cracking of the crystal boule.

3.2. Crystals of 5 cm in diameter

A new Czochralski furnace was set up based on the numerical modeling performed in [6]. This configuration was numerically optimized in order to reduce the thermal stress in the crystals and to avoid that fast crystallization starts from the crucible bottom, which was previously observed during the growth of 3 cm diameter ingots in the non-optimized furnace [6]. The first ingot grown by using the automatic control was 5 cm in diameter and 15 cm in length (Fig. 4b). Numerical results plotted in Fig. 4a show a less curved growth interface by the end of the solidification process (f=1 cm for a solidification length $L_{cyl} = 15$ cm). The radial temperature difference between the crystal center and the periphery near the triple solid-liquid-gas point is ΔT_{rad}=105 K. The crystal boule was free of cracks before and after cutting.

The radial temperature difference in the 3- and 4-cm diameter crystals grown in the non-optimized configuration and, respectively, in the ingot of 5 cm diameter grown in the optimized furnace, are shown in Fig. 5. The temperature difference between the center and the crystal periphery (ΔT_{rad}=105 K) is estimated 0.2 cm above the triple solid-liquid-gas line for a solidified length of the ingot $L_{cyl}\approx$6 cm. The temperature difference increases by 30 K when the diameter of the ingot increases from 3 cm

to 4 cm in the case of the non-optimized configuration: ΔT_{rad}=70 K (d=3 cm) and ΔT_{rad}=102 K (d=4 cm). The radial temperature difference in the 5 cm-diameter ingot grown in the optimized configuration, ΔT_{rad}=100 K, is smaller than the temperature difference in the 4 cm-diameter ingot grown in the non-optimized furnace. Moreover, the tail of the crystal 5 cm in diameter had a conical shape (0.5 cm in height). Therefore, the thermal stresses at the bottom part of the ingot have been decreased in the optimized configuration.

4. Conclusions

Numerical modeling was applied in order to investigate the thermal stresses in Li_2MoO_4 crystals grown in two different Czochralski configurations. The crystal boule 4 cm in diameter grown in the non-optimized furnace cracked during the cutting of the bottom part of the ingot. Numerical results show that high thermal stresses at the bottom part of the ingot are generated by the large radial temperature gradients and by the unusual concave shape of the tail. The furnace configuration used to grow crystals 5 cm in diameter was numerically optimized in order to reduce the thermal stresses. The first kg-mass LMO ingot grown in this furnace was free of cracks and exhibited a regular outer shape.

Acknowledgments

This work is supported by the ANR agency, via the CLYMENE (n° ANR-16-CE08-0018-01) grant. Xuejin Wan is acknowledged for the calculations of the C_{ij} tensor elements.

References

[1] T. B. Bekker *et al.*, Astropart. Phys. 72 (2016) 38-45.

[2] E. Armengaud *et al.*, Eur. Phys. J. C 77 (2017) 785.

[3] M. Velázquez *et al.*, Solid State Sci. 65 (2017) 41.

[4] G. Buşe *et al.*, Nucl. Inst. Meth. A 891 (2018) 87-91.

[5] X. Wan, *Investigations of mechanical and thermodynamic properties of Li_2MoO_4 single crystals*, Internship report, IFCEN/Institut de Chimie de la Matière Condensée de Bordeaux, France, 2017.

[6] C. Stelian *et al.*, J. Cryst. Growth 492 (2018) 6-12.

Figure captions

Figure 1: (a) Photograph of the 230 g Li_2MoO_4 crystal boule (4 cm in diameter and 6 cm in length); (b) Cleavage starting from the bottom part of the ingot.

Figure 2: (a) Temperature field and isotherms (left side) and velocity field (right side) computed for the 4 cm-diameter crystal grown in the non-optimized furnace configuration; (b) Von Mises stress distribution at the surface of the crystal carried out from local 3D computations. The maximum values of the von Mises stress are shown in the x-y and y-z planes.

Figure 3: Von Mises stress distribution in the longitudinal x-y section of the ingot at the end stage of the growth (solidification length L=6.3 cm): (a) Case with a convex shape of the lateral surface of the tail; (b) Case with a concave shape of the lateral surface of the tail and photograph of the cracked bottom part of the ingot.

Figure 4: (a) Temperature field and isotherms (left side) and velocity field (right side) computed for the 5 cm-diameter crystal grown in the numerically optimized furnace configuration (L_{cyl}=15 cm) ; (b) Photograph of the first large mass ingot (820 g) grown in the optimized Czochralski furnace.

Figure 5: Temperature field and isotherms computed for the crystals, 3- and 4-cm diameter grown in the non-optimized configuration, and for the ingot 5 cm in diameter grown in the optimized furnace. The temperature differences between the center and the crystal periphery, estimated at a 0.2 cm distance above the triple solid-liquid-gas line are: ΔT_{rad}=70 K (d=3 cm), ΔT_{rad}=102 K (d=4 cm) and ΔT_{rad}=100 K (d=5 cm). The length of the cylindrical part of the ingots is L_{cyl}=6 cm.

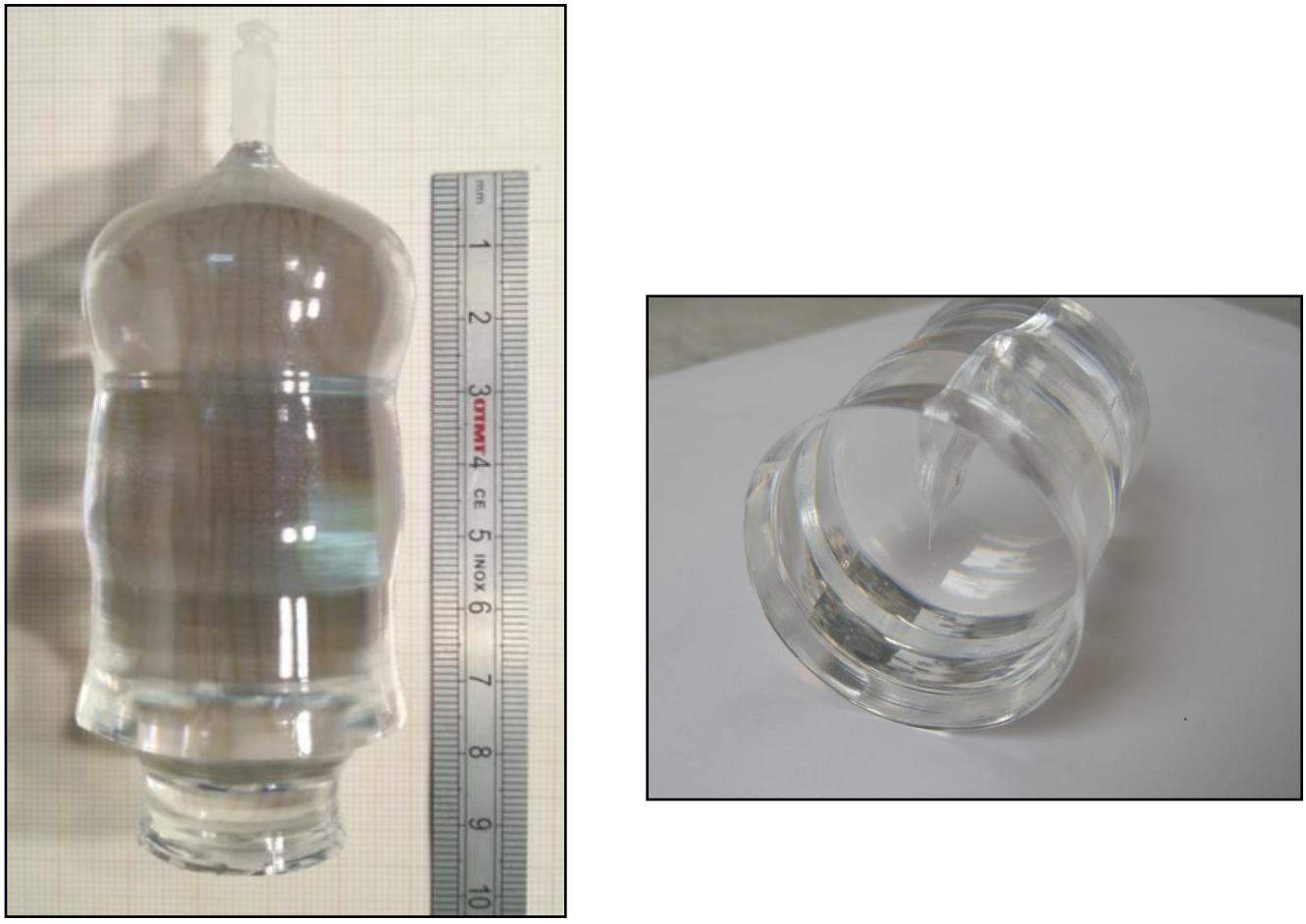

(a) (b)

Figure 1: (a) Photograph of the 230 g Li_2MoO_4 crystal boule (4 cm in diameter and 6 cm in length); (b) Cleavage starting from the bottom part of the ingot.

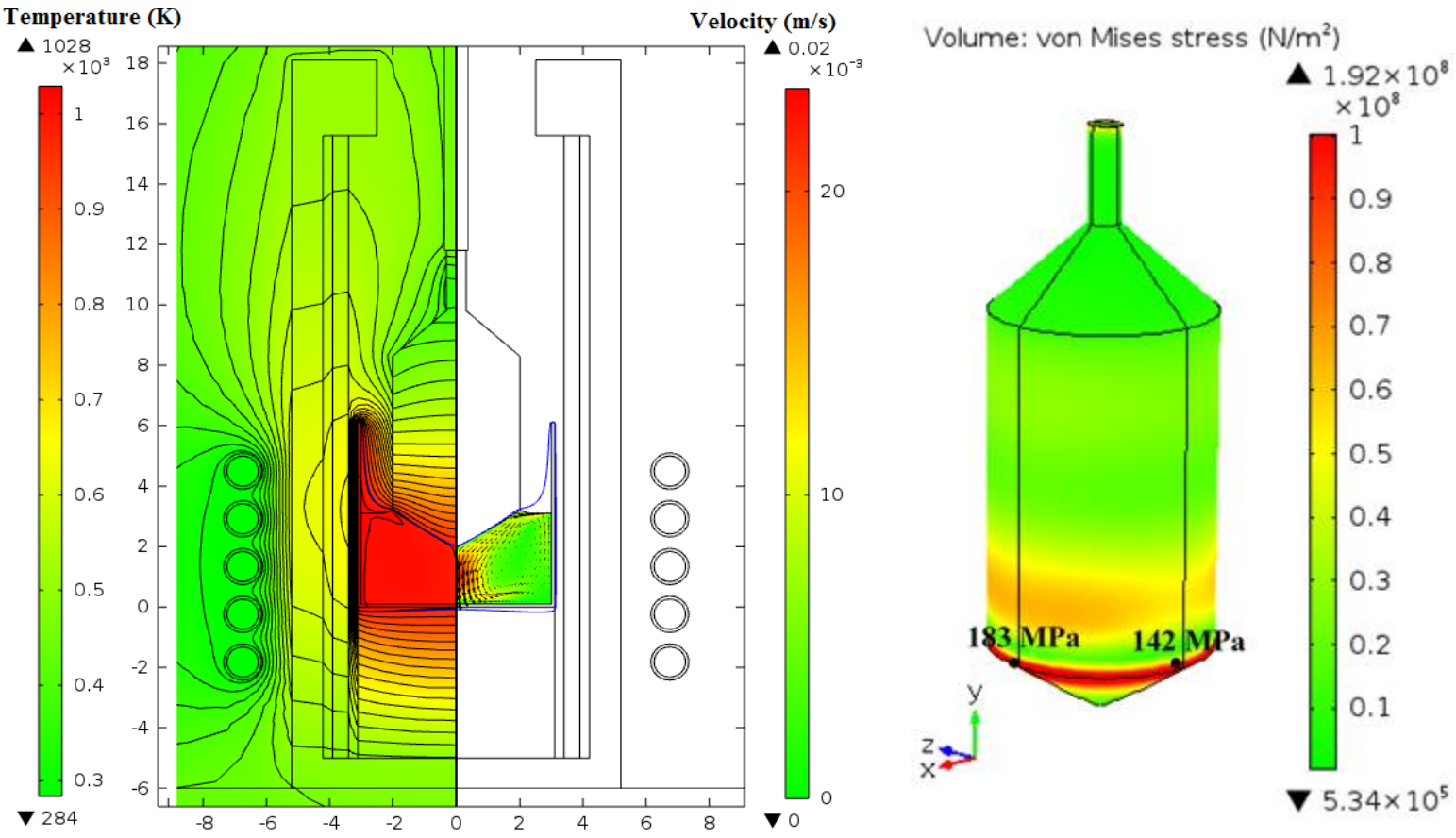

(a) (b)

Figure 2: (a) Temperature field and isotherms (left side) and velocity field (right side) computed for the 4 cm-diameter crystal grown in the non-optimized furnace configuration; (b) Von Mises stress distribution at the surface of the crystal carried out from local 3D computations. The maximum values of the von Mises stress are shown in the x-y and y-z planes.

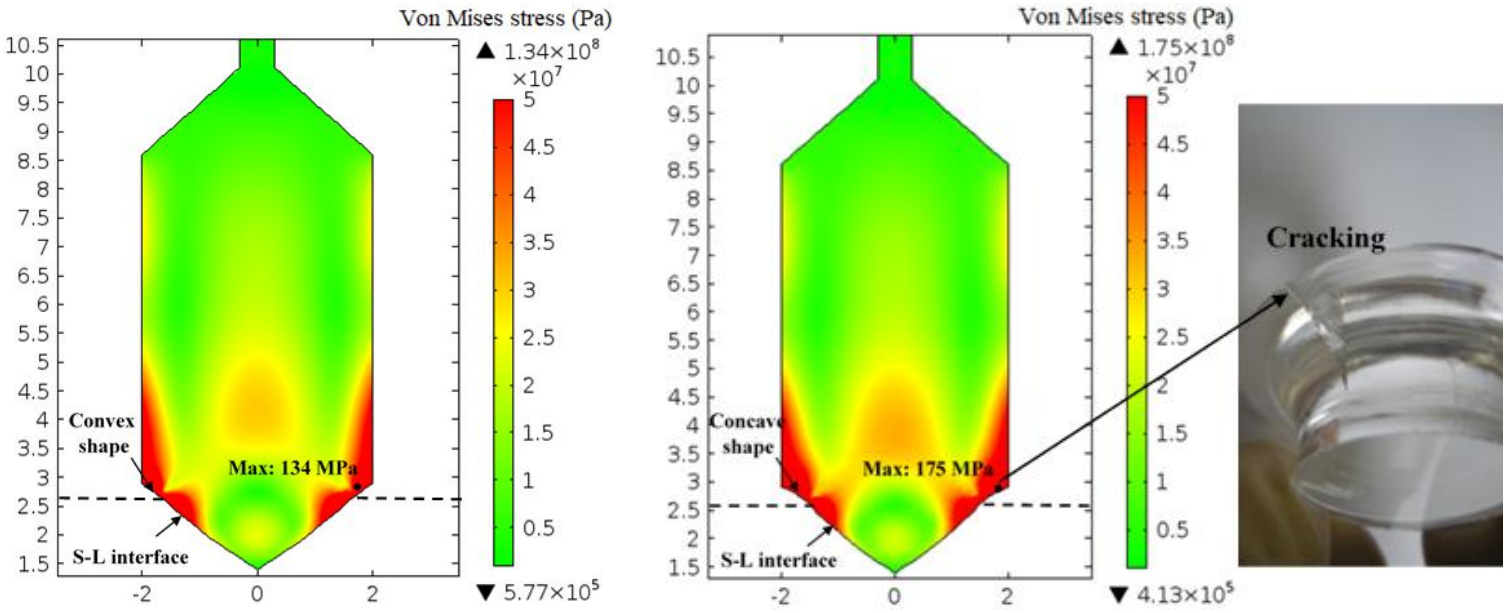

(a) (b)

Figure 3: Von Mises stress distribution in the longitudinal x-y section of the ingot at the end stage of the growth (solidification length L=6.3 cm): (a) Case with a convex shape of the lateral surface of the tail: (b) Case with a concave shape of the lateral surface of the tail and photograph of the cracked bottom part of the ingot.

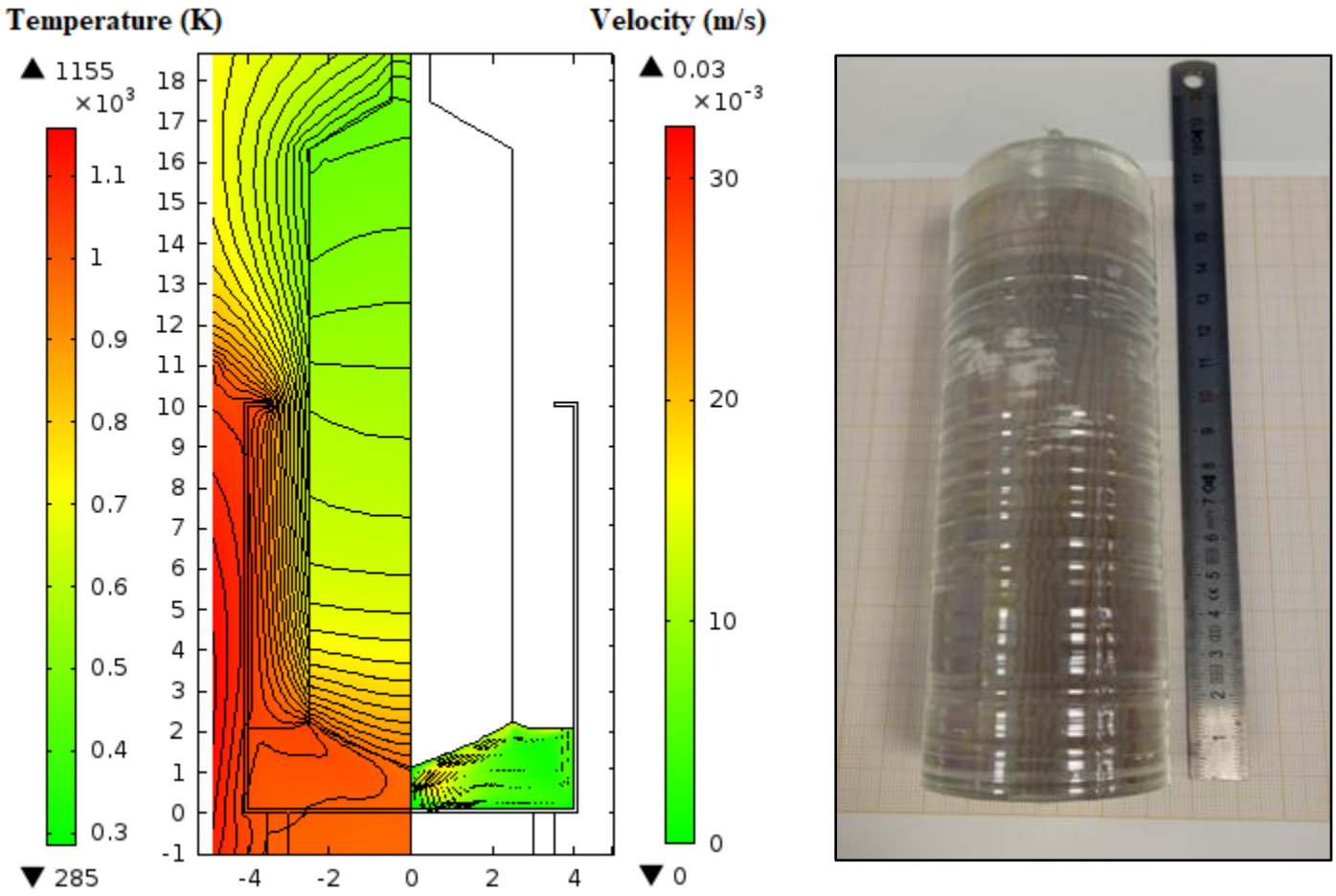

(a) (b)

Figure 4: (a) Temperature field and isotherms (left side) and velocity field (right side) computed for the 5 cm-diameter crystal grown in the numerically optimized furnace configuration (L_{cyl}=15 cm) ; (b) Photograph of the first large mass ingot (820 g) grown in the optimized Czochralski furnace.

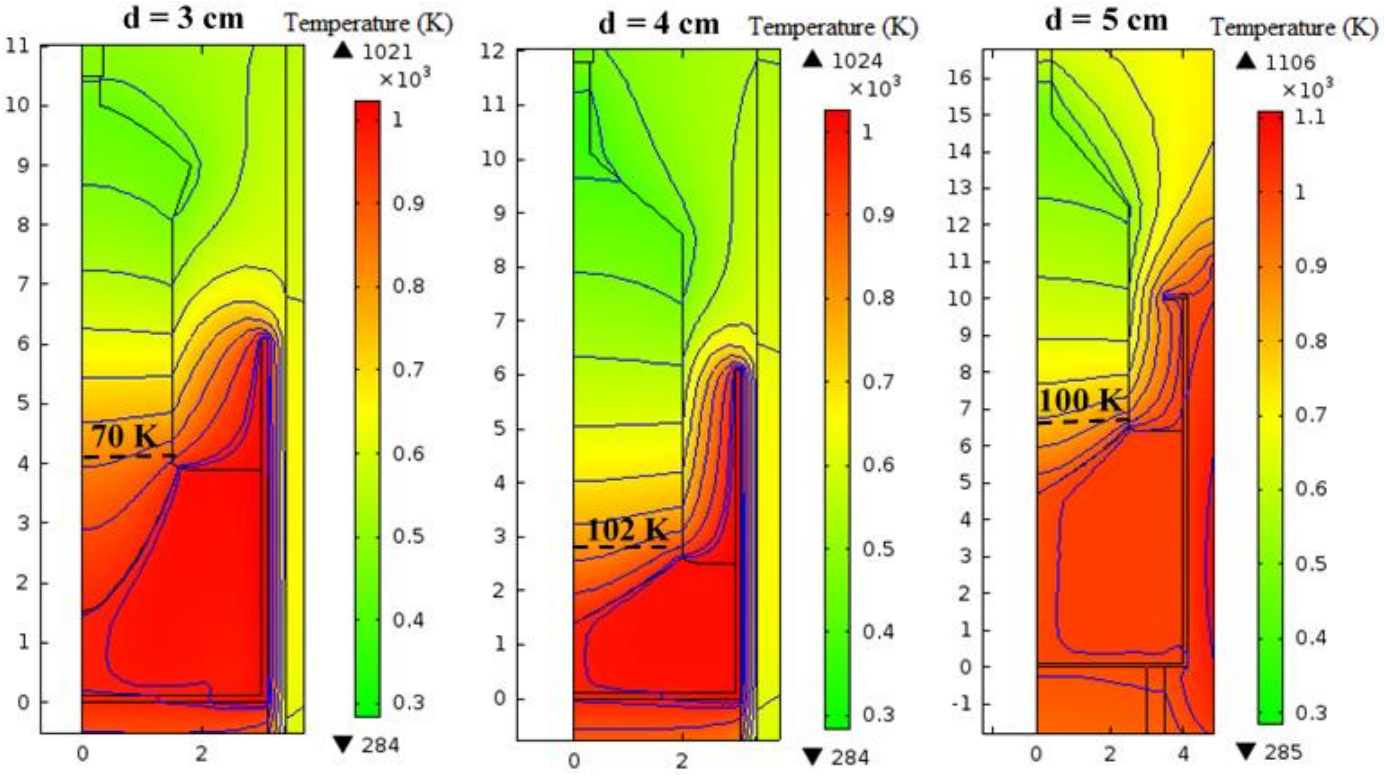

Figure 5: Temperature field and isotherms computed for the crystals, 3- and 4-cm diameter grown in the non-optimized configuration, and for the ingot 5 cm in diameter grown in the optimized furnace. The temperature differences between the center and the crystal periphery, estimated at a 0.2 cm distance above the triple solid-liquid-gas line are: ΔT_{rad}=70 K (d=3 cm), ΔT_{rad}=102 K (d=4 cm) and ΔT_{rad}=100 K (d=5 cm). The length of the cylindrical part of the ingots is L_{cyl}=6 cm.